Interferon-gamma, Interleukin-10, Intercellular Adhesion Molecule-1, and Chemokine Receptor 5, but not Interleukin-4, Attenuate the Development of Periapical Lesions

Andiara De Rossi, DDS, MSc, Lenaldo B. Rocha, DDS, PhD, and Marcos A. Rossi, MD, PhD

Abstract

This study examines the role of Th1 (interferon-gamma [IFN-γ]) and Th2 (interleukin-4 [IL-4] and IL-10) cytokines, an intercellular adhesion molecule (ICAM-1), and a chemokine receptor (CCR5) in the pathogenesis of periapical lesions at different stages of development in knockout mice. For lesion induction, the first molar was opened and inoculated with 4 bacterial strains and left open to the oral environment. After 21 and 42 days, the IFN-γ, IL-10, ICAM-1, and CCR5 knockout animals presented periapical lesions larger than those of wild-type animals. There was no statistically significant difference between periapical lesions induced in IL-4 knockout and wild-type animals during the periods evaluated. Our findings suggest an important role for IFN-γ, IL-10, ICAM-1, and CCR5 in the pathogenesis of experimentally induced pulp infection and bone destruction as endogenous suppressor of periapical lesion development, whereas IL-4 appears to present a nonsignificant effect on periapical lesion modulation. *(J Endod 2008; 34:31–38)*

Key Words

Bone resorption, CCR5, ICAM-1, IFN-γ, IL-4, IL-10, knockout mice, periapical disease

From the Department of Pathology, Faculty of Medicine of Ribeirão Preto, University of São Paulo, Ribeirão Preto, São Paulo, Brazil.

Supported by grants from Fundação de Amparo à Pesquisa do Estado de São Paulo, São Paulo, Brazil (FAPESP 04/03419-3, 06/59618-7, and 07/52556-1), and Conselho Nacional de Desenvolvimento Científico e Tecnológico (M.A.R. is Senior Investigator). This work is part of a doctoral thesis by Andiara De Rossi.

Address requests for reprints to Andiara De Rossi, Department of Pathology, Faculty of Medicine of Ribeirão Preto, University of São Paulo, 14049-900 Ribeirão Preto, SP, Brazil. E-mail address:andiaraderossi@bol.com.br.

0099-2399/$0 - see front matter

doi:10.1016/j.joen.2007.09.021

Bacterially induced bone destruction, including periapical periodontitis (periapical lesion), marginal periodontitis, or osteomyelitis, is the most prevalent skeletal disease (1). Periapical lesions are an expression of the host defensive reaction against bacteria and their toxic components to prevent its dissemination into bone. The host response is complex and involves the recruitment of inflammatory cells and the participation of an extensive network of immunologic mechanisms including the generation of cytokines, the expression of cell surface adhesion molecules, and the production of chemotactic molecules such as chemokines and their receptors, which ultimately result in destruction of alveolar bone (2). Recently, there has been great interest in determining whether these mechanisms protect against bone loss, contribute to its development, or are merely epiphenomenal.

Specific T- and B-cell–mediated antibacterial responses activate a network of regulatory cytokines that are produced by infiltrating T-helper type 1 (Th1) and type 2 (Th2) lymphocytes. Interleukin-1 (IL-1) has been implicated as a central mediator of bone and tissue destruction (3). A model for the operation in periapical lesions predicts that the Th1 subset up-regulates IL-1 and other proinflammatory cytokines, whereas inhibitors of IL-1 are related to the Th2 subset (4, 5). However, some studies have demonstrated that gene knockouts of the Th2-type cytokines IL-10 and to a lesser extent IL-6, but not IL-4, resulted in enhanced periapical bone destruction after infection of the dental pulp (6, 7). Thus, the role of Th1 and Th2 cytokines in periapical lesions is still controversial in the literature.

Chemokines, a family of chemotactic cytokines, attract leukocyte populations to the infection sites by binding to the 7 transmembrane-spanning G-protein coupled receptors CCR1 through CCR8. The interest in the role of CCR5 during the immune response to infectious diseases has emerged because of their function as a co-receptor in human immunodeficiency virus–1 (HIV-1) (8). The CCR5 receptor has also been studied because of therapeutic potential in infectious and allergic pulmonary disease (9). The statement that CCR5 is present in human periapical lesions and not in clinically healthy periodontal ligaments (10) suggests its possible participation in the process of periapical disease.

Migration of various types of lymphocytes from the circulation into sites of infection is mediated not only by specific chemokine receptors but also by adhesion molecules. The intercellular adhesion molecule–1 (ICAM-1) is an immunoglobulin-like cell adhesion molecule expressed by several cell types, including leukocytes and endothelial cells. ICAM-1 on endothelium plays an important role in migration of activated leukocytes to the sites of inflammation and is also important in adaptive immunity. Integrin binding to ICAM-1 is a co-stimulatory signal for T- and B-lymphocyte activation, in addition to their extravasation. Some adhesion molecules and chemokine receptors have been found in diseased human periapical tissues (10, 11), but their role in the pathogenesis of periapical lesions remains to be solved.

The precise role of cytokines, adhesion molecules, and chemokine receptors in stimulation or protection of bone resorption is unknown. The use of genetically engineered models of immunodeficiency is beginning to shed some light on this area. A few studies have been using knockout ($^{-/-}$) animals to investigate isolate mechanisms in

the pathogenesis of periapical disease at restricted stages of development (6, 7, 12, 13), occasionally with conflicting results (6, 14).

In an attempt to better describe the pathogenesis of periapical lesions, it is important to conduct an investigation on the general mechanisms involved in stimulation or protection of bone destruction at different stages of periapical lesion development. This study examines the role of Th1 (interferon-gamma [IFN-γ]) and Th2 (IL-4 and IL-10) cytokines, ICAM-1, and a chemokine receptor (CCR5) in the pathogenesis of periapical lesions at different stages of development by using a well-established in vivo model of periapical disease in knockout mice.

Material and Methods

Animals

All animal procedures performed in this study were in accordance with international guidelines for the use of animals and received prior approval by the Animal Ethics Committee of the Faculty of Medicine of Ribeirão Preto, University of São Paulo. Male C57BL/6 wild-type mice (WT) and mice deficient in IFN-γ, IL-4, IL-10, ICAM-1, and CCR5, 6- to 8-weeks-old in the beginning of the experiments, were used. The mice were bred and maintained in microisolator cages in the animal housing facility of the Department of Pathology, Faculty of Medicine of Ribeirão Preto, University of São Paulo. Mice with targeted disruption of IFN-γ, IL-4, IL-10, ICAM-1, and CCR5 were obtained from Jackson Laboratories (Bar Harbor, ME). All knockout mice were originally generated in a mixed 129-B6-DBA background and then backcrossed to the C57BL/6J background for more than 8 generations.

Periapical Lesion Induction

For lesion induction, mice were anesthetized by intramuscular injection of ketamine (150 mg/kg of body weight) and xylazine (7.5 mg/kg of body weight) and mounted on a jaw retraction board. A classic mouse model of periapical lesion induction was used (6, 7, 13). The mandible first molar pulp chamber was opened by using a variable speed electric dental handpiece with a #1/4 dental round bur until the entrances of the canals could be visualized and probed with a #08 endodontic file. The root canals were directly inoculated with 10 ìL (10^6 bacteria) of a mixture of 4 common endodontic pathogens, *Porphyromonas gingivalis* (ATCC 33277), *Prevotella nigrescens* (ATCC 33563), *Actinomyces viscosus* (ATCC 91014), and *Fusobacterium nucleatum subsp.polymorphum* (ATCC 10953), and then left open to the oral environment. Mice without pulp exposure served as controls.

Histopathologic Analysis

All animals were killed by CO_2 asphyxiation on days 7, 21, or 42 after pulp inoculation. The mandible was removed. After removal of soft tissue, the teeth were separated and individually fixed in 10% phosphate-buffered formalin and demineralized in 4.13% ethylenediaminetetraacetic acid, pH 7.2, at room temperature for 5 weeks. Once decalcified, the specimens were washed in running water for 24 hours, dehydrated in ascending concentrations of ethanol, cleared in xylol, and embedded in paraffin. Longitudinal 5-μm-thick sections were cut in mesiodistal orientation at the tooth apex level, stained with hematoxylin-eosin (HE), modified Brown and Brenn (BB) staining method for gram-positive and gram-negative bacteria (15), and tartrate-resistant acid phosphatase (TRAP) for osteoclast identification (16), and examined under a light and fluorescence microscope (Leica DMR; Leica Microsystem Wetzlar Gmbh, Wetzlar, Germany). All quantitative measurements were made with videomicroscopy with Leica QWin software (Leica Imaging Systems Ltd, Cambridge, UK) in conjunction with the light microscope, videocamera (Leica DC-300F; Leica Microsystems AG, Heerbrugg, Switzerland), and an on-line computer. The sections of each jaw sample containing the distal root of the mandibular first molar and simultaneously showing the coronal and apical pulp through the apical foramen and the connecting periapical tissue were selected for quantitative measurements. For each data point, specimens were obtained from 5 mice.

Morphometric Analysis under Fluorescence Microscopy

Morphometric analysis of periapical lesion size was performed in tissue sections stained with HE, with the microscope operating in fluorescence mode (17). Measurements were restricted to histologic sections representing the maximum lesion size. A skilled observer masked to the specimen strain performed all morphometric procedures. Delineation was performed excluding intact tooth and bone structures and including the inflammatory infiltrate areas. If necessary, the observer could manipulate image characteristics of brightness, contrast, and magnification to improve the visualization of the inflamed areas of the periapical lesions in tissue sections.

Polymorphonuclear Leukocyte Recruitment

The number of polymorphonuclear leukocytes was counted under conventional light microscopy. A counting frame was centered at a fixed distance from the apical foramina of distal roots throughout the selected section of each different specimen of the HE-stained slides. Within these designated areas, the number of polymorphonuclear leukocytes was counted by using their identifying characteristics such as darkly stained cells with multilobed, horseshoe-shaped nuclei.

Bacterial Penetration of Tissues

Bacterial penetration in tissue sections stained with a modified BB technique (15) was assessed under conventional light microscopy. The tissues within the root canal were divided into 3 equal parts: coronal third, middle third, and apical third. The following scale was used to assess the bacterial penetration from coronal to apical third: 0, no bacteria; 1, bacteria in the coronal third; 2, bacteria in the middle third; 3, bacteria in the apical third; 4, bacteria in the periapical lesion. The highest score represented the bacterial status of that canal.

Osteoclastogenesis (TRAP Assay)

Osteoclastogenesis was measured as the number of osteoclasts per millimeter length of resorbed bone. TRAP is a histochemical marker of osteoclasts (16). Deparaffinized sections were incubated in a solution prepared by dissolving 8 mg of naphtol AS-BI (Sigma Chemical Co, St Louis, MO) in 500 μL of N-N-dimethylformamide followed by the addition of 50 mL of 0.2 mol/L sodium acetate buffer (pH 5.0) and 70 mg of Fast Red Salt TR (Sigma Chemical Co). Sodium tartrate dihydrate (50 mmol/L) was added to the solution. After incubation at 37°C, the sections were washed in distilled water and stained with hematoxylin. TRAP-positive cells appeared red. As a control of specificity for TRAP activity, sections were incubated in substrate-free medium. The quantitative analysis of the number of TRAP-positive osteoclasts was determined by counting multinucleated TRAP-positive cells in direct contact with bone on the light microscope and expressed as the number per millimeter of bone length. The surface of the alveolar bone was measured with the image analysis system.

Statistical Analysis

Data were analyzed with the GraphPad Prism software (Prism, Chicago, IL). One-way analysis of variance and the Dunnett test (for multiple comparisons) were used to evaluate the differences between the means of periapical lesion dimension at days 7, 21, and 42 after procedures. A level of significance of 5% was chosen to denote the

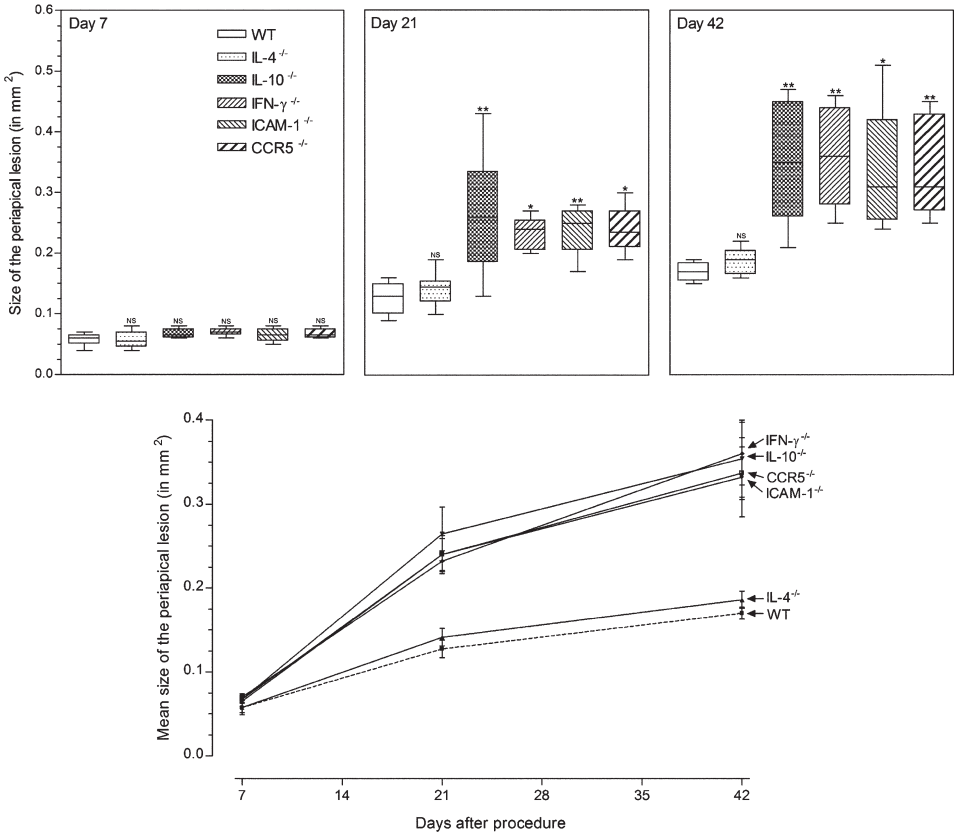

Figure 1. Values represent the mean size ± SEM of the periapical lesion around the distal root of mandibular first molar determined at days 7, 21, and 42 after coronal opening and contamination of the root canal from WT and IFN-γ, IL-4, IL-10, ICAM-1, and CCR5 knockout ($^{-/-}$) mice. NS, not significant. *$P < .05$; **$P < .01$.

difference between group means. Data are presented as mean ± standard error of the mean (SEM).

Results

Histopathologic and Morphometric Analysis

At day 7, the qualitative analysis revealed that all specimens appeared similar, with pulp necrosis mainly at the coronal and middle thirds of the root canal. A thin layer of inflammatory cells, composed of neutrophils and lymphomononuclear cells, capped the periapical region. The neutrophils were the most prevalent cells, mainly concentrated in the apical third of the root and adjacent to the apex. The use of fluorescence microscopy allowed adequate resolution of the periapical lesion, clearly detected and delineated; the periodontal ligament appeared completely destroyed at the bone side, and ligament fibers remained attached to the cementum. Quantitatively, the mean size of the periapical lesion, in mm^2, was similar in all strains: 0.06 ± 0.01, 0.06 ± 0.01, 0.07 ± 0.01, 0.07 ± 0.01, 0.06 ± 0.01, and 0.07 ± 0.01 in WT, IL-$4^{-/-}$, IL-$10^{-/-}$, IFN-$\gamma^{-/-}$, ICAM-$1^{-/-}$, and CCR$5^{-/-}$ animals, respectively (Fig. 1). Although microabscesses near the apical aperture could be seen in all specimens, the proportion of cells of the periapical lesions varied according to the strains. The absolute number of neutrophils, associated with relative increase in the number of mononuclear cells, was similarly decreased in IL-$10^{-/-}$ (38.50 ± 1.32), IFN-$\gamma^{-/-}$ (38.00 ± 2.00), and ICAM-$1^{-/-}$ (38.10 ± 1.76) mice in comparison with the amount of neutrophils in the lesions in WT (51.67 ± 1.20) and IL-$4^{-/-}$ (51.25 ± 1.25) mice. In contrast, the number of neutrophils, with a relatively decreased amount of lymphomononuclear cells, was increased in CCR$5^{-/-}$ (73.59 ± 5.01) mice as compared with WT controls (Fig. 2).

At day 21, the specimens from all strains presented complete pulp necrosis, with root canals containing remnants of necrotic pulp tissue and debris. The surface of the root apex was occasionally corrugated with lacunae, indicating initial cementum resorption. The mean size of

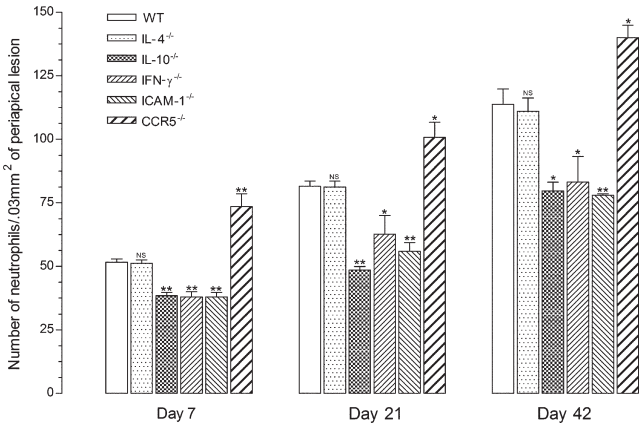

Figure 2. The number of polymorphonuclear leukocytes was counted at days 7, 21, and 42 after coronal opening and contamination of the root canal from WT and IFN-γ, IL-4, IL-10, ICAM-1, and CCR5 knockout ($^{-/-}$) mice. A counting frame (0.02 or 0.03 mm^2) was centered at a fixed distance from the apical foramina of distal roots. Within these designated areas, the number of polymorphonuclear leukocytes was counted by using their identifying characteristics such as darkly stained cells with multilobed, horseshoe-shaped nuclei. Values represent the mean ± SEM per 0.03 mm^2 of bone lesion. NS, not significant. *$P < .05$; **$P < .01$.

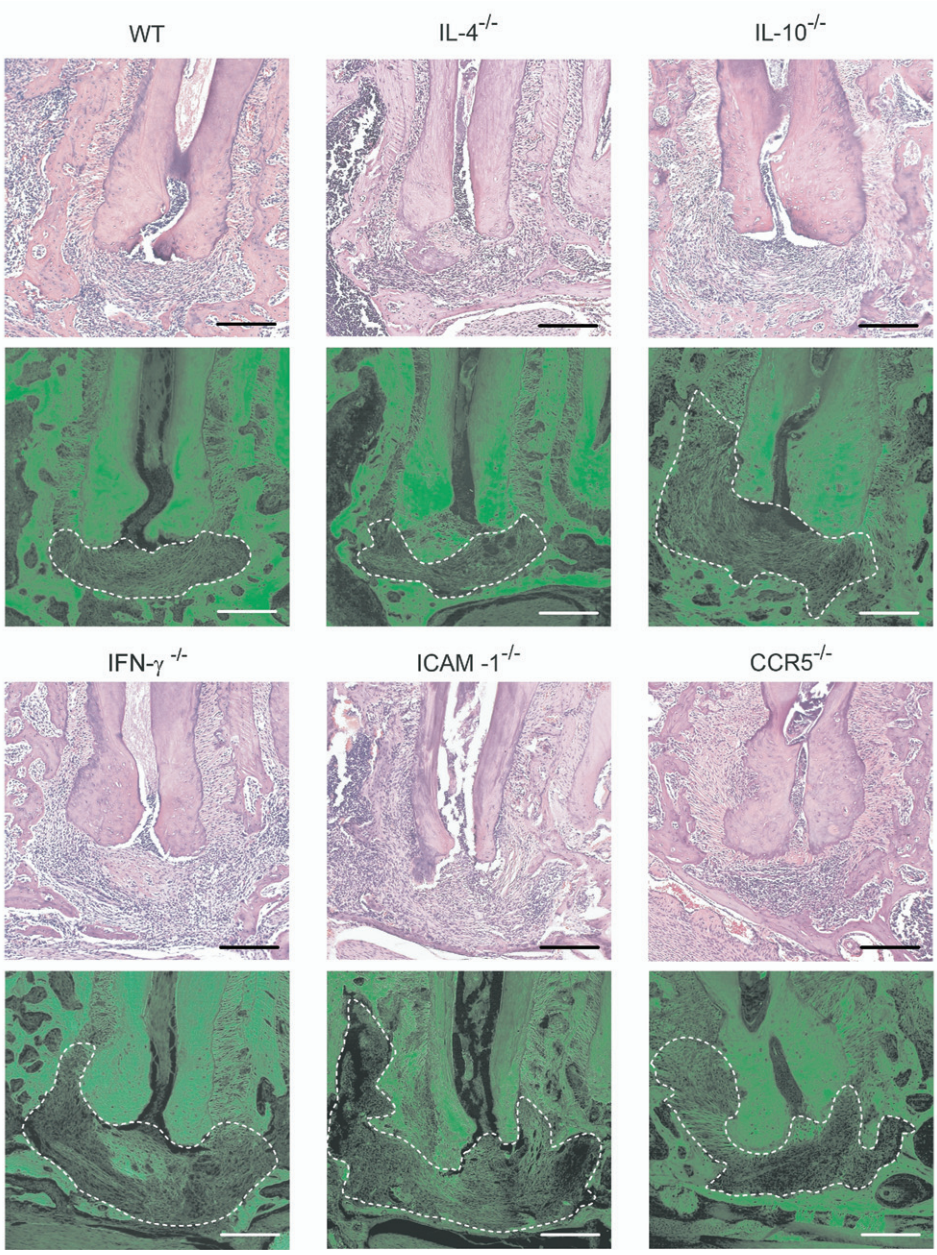

Figure 3. Conventional light and fluorescence microscopy of representative views of the periapical lesions in distal root of mandibular first molar at day 21 after crown access and contamination of the root canal from WT and IFN-γ, IL-4, IL-10, ICAM-1, and CCR5 knockout ($^{-/-}$) mice (HE; bars = 200 μm).

the periapical lesion in IL-$4^{-/-}$ mice (0.14 ± 0.01) was similar to that of WT controls (0.13 ± 0.01), whereas those of IL-$10^{-/-}$ (0.26 ± 0.03), IFN-$\gamma^{-/-}$ (0.23 ± 0.01), ICAM-$1^{-/-}$ (0.24 ± 0.02), and CCR$5^{-/-}$ mice (0.24 ± 0.02) were 120%, 93%, 100%, and 100%, respectively, larger than that of WT controls. Fig. 3 is representative of conventional light and fluorescence microscopy of the periapical lesions at day 21. Although microabscesses near the apical aperture could be seen in all specimens, the proportion in cells of the periapical lesions varied according to the strains. The absolute number of neutrophils, with relative increase in the number of mononuclear cells, was similarly decreased in IL-$10^{-/-}$ (48.50 ± 1.44), IFN-$\gamma^{-/-}$ (62.72 ± 7.28), and ICAM-$1^{-/-}$ (56.00 ± 3.34) mice as compared with the amount of neutrophils in the lesions in both WT (81.50 ± 2.02) and IL-$4^{-/-}$ (81.25 ± 2.28) mice. In contrast, the number of neutrophils, with a relatively decreased number of lymphomononuclear cells, was increased in CCR$5^{-/-}$ (100.80 ± 5.96) mice as compared with WT mice (Fig. 2).

At day 42, specimens from all strains presented root canals containing remnants of necrotic pulp tissue and debris. The surface of the root apex was corrugated with large lacunae, indicating advanced cementum resorption. The mean size of the periapical lesions in IL-$4^{-/-}$ mice (0.19 ± 0.01) was similar to that of WT controls (0.17 ± 0.01), whereas those of IL-$10^{-/-}$ (0.35 ± 0.04), IFN-$\gamma^{-/-}$ (0.36 ± 0.04), ICAM-$1^{-/-}$ (0.33 ± 0.05), and CCR$5^{-/-}$ mice (0.34 ± 0.03) were 108%, 112%, 94%, and 94%, respectively, larger than that of WT controls (Fig. 1). Although microabscesses near the apical aperture could be seen in all specimens, the proportion of cells of the periapical lesions varied according to the strains. The absolute number of neutrophils, with relative increased number of mononuclear cells, was similarly decreased in IL-$10^{-/-}$ (79.67 ± 3.48), IFN-$\gamma^{-/-}$ (83.20 ± 10.07),

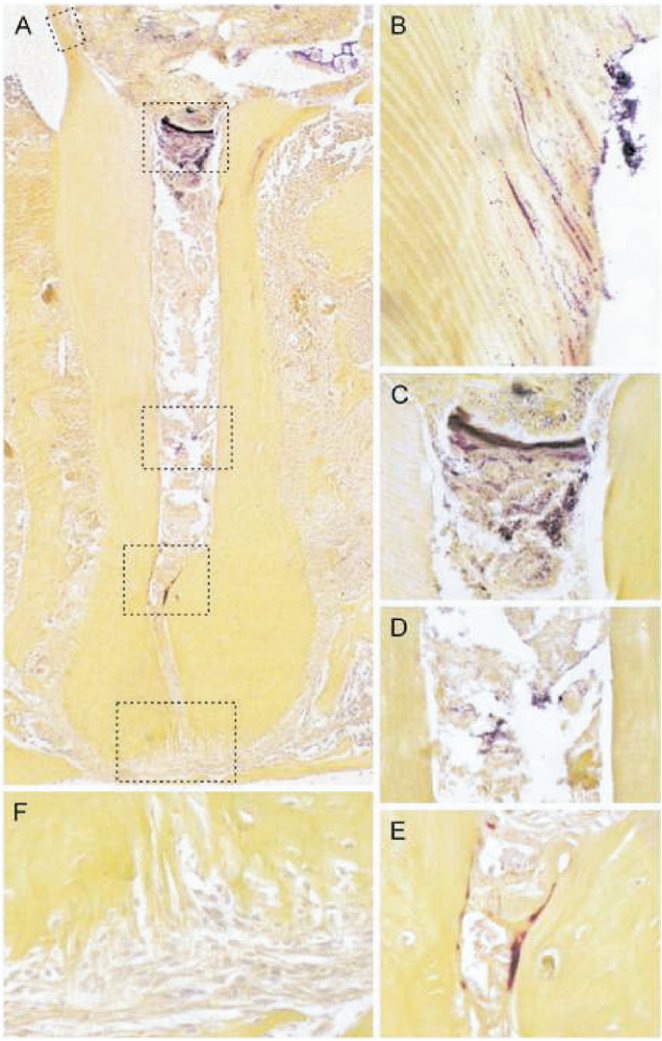

Figure 4. Representative view of the bacterial penetration after crown access and contamination of the root canal (*A*). At all periods, gram-positive (blue) and gram-negative (red) bacteria were found in abundance at the coronal portion of the dental pulp, dentinal tubules (*B*), and cervical third of the root (*C*), in less number at medium third of the root (*D*), penetrated until the end of the root canal (*E*), and were absent in periapical lesion (*F*). There was no significant difference in bacterial penetration of the tissues between all strains at 7, 21, and 42 days after crown access and contamination of the root canal (BB staining; bar: in (*A*) = 500 μm and in (*B–F*) = 10 μm).

and ICAM-$1^{-/-}$ (78.00 ± 0.57) mice as compared with the amount of neutrophils in the lesion in WT (113.80 ± 6.00) and IL-$4^{-/-}$ (111.00 ± 5.29) mice. In contrast, the number of neutrophils, with a relatively decreased amount of lymphomononuclear cells, was augmented in CCR$5^{-/-}$ (140.00 ± 4.89) mice as compared with WT controls (Fig. 2).

Bacterial Penetration of Tissues

There was no significant difference in bacterial penetration of the tissues between WT and all knockout animals at days 7, 21, and 42 after pulp exposure and inoculation. In all periods, all strains were included in score 3; gram-positive and gram-negative bacteria were found in abundance at the coronal portion of the dental pulp and in dentinal tubules and in less numbers at the medium and apical thirds of the root canal. In all specimens bacteria were absent in periapical lesion. Fig. 4 is representative of the bacterial status of periapical lesions at day 7.

Osteoclastogenesis (TRAP assay)

There was no significant difference in number of TRAP-positive cells between WT and all knockout animals. The mean number of TRAP-positive cells per millimeter length of resorbed bone was climaxed at day 7: 5.86 ± 0.43, 7.97 ± 0.937, 6.55 ± 0.68, 6.66 ± 0.33, 6.55 ± 0.35, and 6.62 ± 0.24 in WT, IL-$4^{-/-}$, IL-$10^{-/-}$, IFN-$\gamma^{-/-}$, ICAM-$1^{-/-}$, and CCR$5^{-/-}$ animals, respectively. At 21 days the number of TRAP-positive cells similarly decreased: 3.95 ± 0.52, 4.53 ± 0.21, 3.72 ± 0.53, 4.02 ± 0.83, 3.24 ± 0.38, and 3.64 ± 0.24 in WT, IL-$4^{-/-}$, IL-$10^{-/-}$, IFN-$\gamma^{-/-}$, ICAM-$1^{-/-}$, and CCR$5^{-/-}$ animals, respectively. At 42 days even fewer TRAP-positive cells could be observed in the lesion site: 3.06 ± 0.20, 3.55 ± 0.21, 2.75 ± 0.36, 2.37 ± 0.42, 3.46 ± 0.63, and 3.24 ± 0.55 in WT, IL-$4^{-/-}$, IL-$10^{-/-}$, IFN-$\gamma^{-/-}$, ICAM-$1^{-/-}$, and CCR$5^{-/-}$ animals, respectively (Fig. 5).

Discussion

The inflammatory response is controlled by a network of regulatory cytokines produced by Th1- and Th2-type lymphocytes and adhesion and chemotactic molecules. In the present work we examined development of periapical lesions in knockout mice for the central Th1 cytokine, IFN-γ, the central Th2 cytokines, IL-4 and IL-10, an adhesion molecule, ICAM-1, and a chemokine receptor, CCR5, aiming to estab-

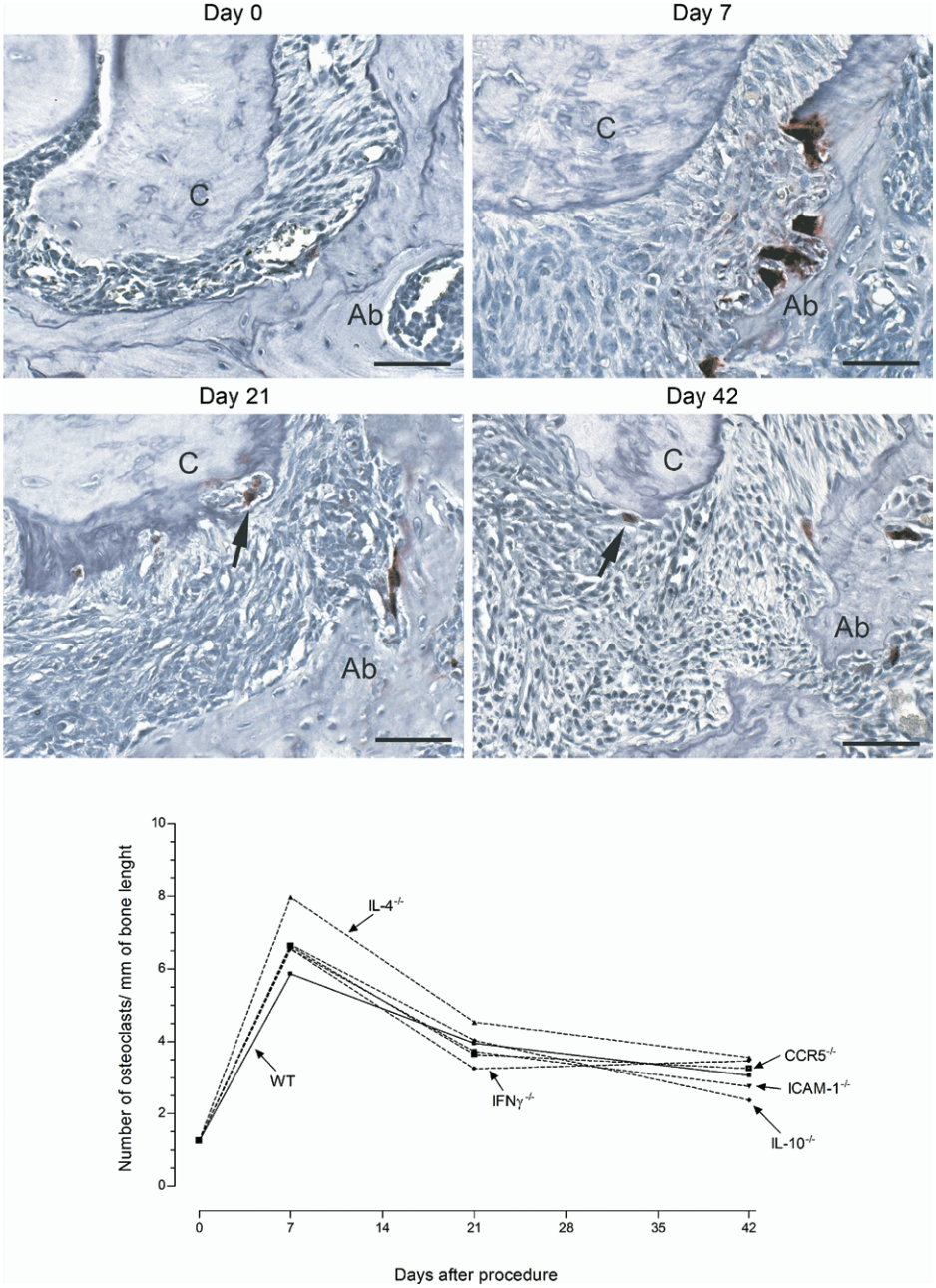

Figure 5. Representative views of the osteoclasts, identified as TRAP-positive multinucleated cells, lining alveolar bone in intact teeth (day 0) and at days 7, 21, and 42 after crown access and contamination of the root canal. The number of osteoclasts was climaxed on day 7. At day 21 the number of osteoclasts decreased, and at day 42 fewer TRAP-positive cells could be observed (TRAP, bars = 100 μm). Osteoclastogenesis was measured as the number of osteoclasts per millimeter of resorbed bone length. Values represent the mean ± SEM. In all strains osteoclastogenesis increased dramatically by day 7 and decreased gradually at days 21 and 42. At any time point, there was no significant difference in number of osteoclasts between all strains.

lish whether such responses are predominantly protective or destructive regarding bone resorption after dental pulp infection.

The mice model of coronal opening followed by inoculation of endodontic pathogens and then left open to the oral environment has been shown to be effective for the experimental induction of periapical inflammation and bone destruction (6, 7, 13). In our study, bacteria were observed in the root canal system of all animals, whereas the obtained periapical lesion was free of bacteria. It is very likely that the defense system mobilized by periapical inflammation first eliminates the bacteria that invade the periapex; the presence of the inflammatory infiltrate resulted from the penetration of bacterial by-products. The modification of the BB technique used in the current study (15) allowed excellent stainability, because it was possible to identify and discriminate bacterial profiles along the teeth.

Th1 and Th2 Cytokines

Both proinflammatory Th1 and anti-inflammatory Th2 cytokines might modulate IL-1 expression, implicated as central mediators of periapical bone resorption and activity by macrophages (5). A model for the operation in periapical lesions predicts that the Th1 subset up-regulates IL-1 and other proinflammatory cytokines, whereas inhibitors of IL-1 are related to the Th2 subset (4, 5). We tested the hypoth-

esis that IFN-γ, the major product of activated Th1 cells, would enhance periapical inflammation and bone resorption adjacent to sites of infection. Our findings, however, could show that IFN-$\gamma^{-/-}$ mice developed greater periapical lesions than WT controls at days 21 and 42, suggesting that, at least individually, endogenous IFN-γ might have protective effect on the pathogenesis of late periapical bone resorption in vivo. Recently, it has been proposed that IFN-γ is critical for the suppression of pathologic bone resorption associated with inflammation because it inhibits osteoclastogenesis by interfering with the receptor activator for nuclear factor-κB ligand (RANKL)-RANK signaling pathway and inducing rapid degradation of tumor necrosis factor receptor–associated factor 6 (18). Conversely, previous investigation suggested that IFN-$\gamma^{-/-}$ mice do not have significantly reduced infection-simulated bone resorption, possibly as a result of functional redundancy in proinflammatory pathways (13). Moreover, our findings also demonstrated that the Th2 cytokines, IL-4 and IL-10, exhibited different functions in bone destruction modulation; IL-$10^{-/-}$ mice developed greater periapical lesions than those in IL-$4^{-/-}$ mice, and these latter were quite similar to the lesions induced in WT animals. Functional discordance among the Th2-type cytokines was previously pointed out; IL-$10^{-/-}$, but not IL-$4^{-/-}$, mice exhibited enhanced periapical bone destruction after infection of the dental pulp (6). By contrast, mice immunized to develop strong and polarized Th1 response developed an extensive inflammation associated with alveolar bone destruction heavily infiltrated with osteoclasts, whereas Th2-biased mice and controls developed minimal lesions and no obvious osteoclasts (14).

ICAM-1

Although adhesion molecules have been observed in human periapical lesions (11), their implication in its pathogenesis has not been evaluated. Endothelial ICAM-1 plays a key role in leukocyte migration to the site of infection. We tested and confirmed the hypothesis that ICAM-1 deficiency results in compromised immune response reflected by enhanced periapical inflammation and bone resorption. Correspondingly, P/E selectin knockout mice, which lack rolling adhesion of leukocyte to endothelium, also presented increased bone destruction and higher levels of the bone resorptive cytokine, IL-1α, in the periapical inflammatory sites (19). A study from our laboratory demonstrated that ICAM-1 is effectively involved in the early formation of granulomas and participates in the resistance of mice to infection with the fungus *Paracoccidioides brasiliensis*; the absence of ICAM-1 resulted in decreased number of CD4 and CD8 T cells and increased production of IL-4 in the inflammatory site (20).

CCR5

Once CCR5 receptor is critical mediator of leukocyte trafficking and activation, we tested the hypothesis that the absence of this receptor results in compromised immune response in periapical lesion development. Our results clearly showed that CCR$5^{-/-}$ mice developed greater periapical lesions at days 21 and 42 after procedure in comparison with WT controls and exhibited a more pronounced neutrophilic infiltrate, thus suggesting a role for CCR5 in periapical bone resorption. Similarly, a recent study demonstrated that CCR$5^{-/-}$ mice developed a more severe pancreatic injury than WT mice during cerulein-induced acute pancreatitis as assessed by a more severe inflammatory infiltrate, mainly neutrophilic (21). However, the precise mechanism by which CCR5 can modulate the immune response in periapical lesion has to be determined.

Polymorphonuclear Leukocyte Recruitment

Polymorphonuclear neutrophils are usually thought of as the leukocyte population involved in acute inflammatory responses, acting as first line of defense against invading microorganisms. On the other hand, recent findings have shown that these cells are able to synthesize cytokines in response to a variety of inflammatory stimuli (22). According to our results, periapical lesions occurred as a tissue reaction to bacterial infection and consisted of inflammatory cell infiltration, mainly composed of neutrophils at all stages of development. These findings place neutrophils at a pivotal position in which they regulate not only acute inflammatory reaction but also the chronic inflammatory response in the present case, as understood as a long-term persistent infection caused by root canals left opened to the oral environment. A negative correlation between the extent of periapical lesions and the number of neutrophils was demonstrated in WT and IFN-γ, IL-4, IL-10, and ICAM-1 knockout animals, suggesting a protective role of neutrophils in the control of infection-stimulated alveolar bone resorption in this model. The role of neutrophils in defense against bacteria in pulpal tissue was previously demonstrated in rats (23). However, an exception was observed for CCR$5^{-/-}$ animals; a larger periapical lesion was correlated with an increase in the number of neutrophils during all periods. The higher number of neutrophils in these animals could be ascribed to the abrogated recruitment of monocytes caused by CCR5 deficiency, the main receptor for macrophage inflammatory protein-1α (MIP-1α) (24). In addition, the degranulation of neutrophils could be implicated in connective tissue destruction. In rats, the methotrexate-induced neutropenia elicited after pulpal exposure did not change the status of the periapical lesion, whereas the neutropenia before the exposure inhibited the infiltration of inflammatory cells, especially that by neutrophils, into the lesion and the development of the periapical lesion (25). This finding suggests that neutrophils infiltrated in periapical tissue initiate the development of the periapical lesion. Further studies are needed to elucidate the protective or destructive role of neutrophils in acute and chronic stages of periapical lesions in this model, possibly by use of knockout mice with experimentally induced neutropenia.

Osteoclastogenesis (TRAP Assay)

Microscopic examination of TRAP-stained sections demonstrated that the osteoclast number proceeded rapidly for all strains at day 7 and then gradually decreased at days 21 and 42. This decrease in the number of TRAP-positive cells contrasting with the increased size of the lesion was also reported in periapical lesions induced in IL-1 and/or tumor necrosis factor (TNF) knockout mice (26) and in normal rats and correlated to a decrease in the expression of receptor activator of RANKL (27). Synergic effects of RANKL and proinflammatory cytokine signaling are considered to be induced in the periapical area in response to bacterial stimuli, which would be responsible for the progress of periapical lesion expansion. On the other hand, the synthesis of negative regulators of RANKL and proinflammatory cytokines is rapidly induced with lesion progression (28). This negative response would control the severe progress of bone destruction and inflammatory disease. Further studies are needed to reveal the components and functions of the mediator network correlated with the progress of periapical bone destruction.

Conclusion

Multiple mechanisms are involved in the pathologic changes associated with acute and chronic periapical lesions. Our results suggest that at least individually, IFN-γ, IL-10, ICAM-1, and CCR5 play an important role in the pathogenesis of experimentally induced pulp infection as endogenous suppressor of periapical lesion development, whereas IL-4 did not present significant effect on periapical lesion modulation. Further studies are in progress to elucidate the intrinsic mechanism implicated in the development of perapical lesions, such as the

determination of the levels of proinflammatory and anti-inflammatory cytokines, the regulation of IL-1 production, and regulatory mechanisms governing osteoclast activity. The investigation of the dynamic equilibrium between defensive and destructive mechanisms might provide a pathologic basis for better understanding of the clinical signs and symptoms of pathologic bone resorption associated with inflammation, possibly influencing treatment strategy and shedding some light on the mechanism of bone destruction.

Acknowledgments

The authors thank Maria Elena Riul for excellent technical assistance.

References

1. Nair SP, Meghji S, Wilson M, Reddi K, White P, Henderson B. Bacterially induced bone destruction: mechanisms and misconceptions. Infect Immun 1996;64:2371–80.
2. Stashenko P, Yu SM, Wang CY. Kinetics of immune cell and bone resorptive responses to endodontic infections. J Endod 1992;18:422–6.
3. Wang CY, Stashenko P. The role of interleukin-1 alpha in the pathogenesis of periapical bone destruction in a rat model system. Oral Microbiol Immunol 1993;8:50–6.
4. Stashenko P, Teles R, D'Souza R. Periapical inflammatory responses and their modulation. Crit Rev Oral Biol Med 1998;9:498–521.
5. Kawashima N, Stashenko P. Expression of bone-resorptive and regulatory cytokines in murine periapical inflammation. Arch Oral Biol 1999;44:55–66.
6. Sasaki H, Hou L, Belani A, et al. IL-10, but not IL-4, suppresses infection-stimulated bone resorption in vivo. J Immunol 2000;165:3626–30.
7. Balto K, Sasaki H, Stashenko P. Interleukin-6 deficiency increases inflammatory bone destruction. Infect Immun 2001;69:744–50.
8. Wu L, LaRosa G, Kassam N, et al. Interaction of chemokine receptor CCR5 with its ligands: multiple domains for HIV-1 gp120 binding and a single domain for chemokine binding. J Exp Med 1997;186:1373–81.
9. Hogaboam CM, Carpenter KJ, Schuh JM, Proudfoot AA, Bridger G, Buckland KF. The therapeutic potential in targeting CCR5 and CXCR4 receptors in infectious and allergic pulmonary disease. Pharmacol Ther 2005;107:314–28.
10. Kabashima H, Yoneda M, Nagata K, et al. The presence of chemokine receptor (CCR5, CXCR3, CCR3)-positive cells and chemokine (MCP1, MIP-1alpha, MIP-1beta, IP-10)-positive cells in human periapical granulomas. Cytokine 2001;16:62–6.
11. Kabashima H, Nagata K, Maeda K, Iijima T. Involvement of substance P, mast cells, TNF-alpha and ICAM-1 in the infiltration of inflammatory cells in human periapical granulomas. J Oral Pathol Med 2002;31:175–80.
12. Hou L, Sasaki H, Stashenko P. Toll-like receptor 4-deficient mice have reduced bone destruction following mixed anaerobic infection. Infect Immun 2000;68:4681–7.
13. Sasaki H, Balto K, Kawashima N, et al. Gamma interferon (IFN-gamma) and IFN-gamma-inducing cytokines interleukin-12 (IL-12) and IL-18 do not augment infection-stimulated bone resorption in vivo. Clin Diagn Lab Immunol 2004;11:106–10.
14. Stashenko P, Goncalves RB, Lipkin B, Ficarelli A, Sasaki H, Campos-Neto A. Th1 immune response promotes severe bone resorption caused by *Porphyromonas gingivalis*. Am J Pathol 2007;170:203–13.
15. Taylor RD. Modification of the Brown and Brenn gram stain for the differential staining of gram-positive and gram-negative bacteria in tissue sections. Am J Clin Pathol 1966;46:472–4.
16. Minkin C. Bone acid phosphatase: tartrate-resistant acid phosphatase as a marker of osteoclast function. Calcif Tissue Int 1982;34:285–90.
17. De Rossi A, Rocha LB, Rossi MA. Application of fluorescence microscopy on hematoxylin and eosin-stained sections of healthy and diseased teeth and supporting structures. J Oral Pathol Med 2007;36:377–81.
18. Takayanagi H, Sato K, Takaoka A, Taniguchi T. Interplay between interferon and other cytokine systems in bone metabolism. Immunol Rev 2005;208:181–93.
19. Kawashima N, Niederman R, Hynes RO, Ullmann-Cullere M, Stashenko P. Infection-stimulated infraosseus inflammation and bone destruction is increased in P-/E-selectin knockout mice. Immunology 1999;97:117–23.
20. Moreira AP, Campanelli AP, Cavassani KA, et al. Intercellular adhesion molecule-1 is required for the early formation of granulomas and participates in the resistance of mice to the infection with the fungus *Paracoccidioides brasiliensis*. Am J Pathol 2006;169:1270–81.
21. Moreno C, Nicaise C, Gustot T, et al. Chemokine receptor CCR5 deficiency exacerbates cerulein-induced acute pancreatitis in mice. Am J Physiol Gastrointest Liver Physiol 2006;291:1089–99.
22. Kasama T, Miwa Y, Isozaki T, Odai T, Adachi M, Kunkel SL. Neutrophil-derived cytokines: potential therapeutic targets in inflammation. Curr Drug Targets Inflamm Allergy 2005;4:273–9.
23. Nakamura K, Yamasaki M, Nishigaki N, et al. Effect of methotrexate-induced neutropenia on pulpal inflammation in rats. J Endod 2002;28:287–90.
24. Goser S, Ottl R, Brodner A, et al. Critical role for monocyte chemoattractant protein-1 and macrophage inflammatory protein-1alpha in induction of experimental autoimmune myocarditis and effective anti-monocyte chemoattractant protein-1 gene therapy. Circulation 2005;29:3400–7.
25. Yamasaki M, Kumazawa M, Kohsaka T, Nakamura H. Effect of methotrexate-induced neutropenia on rat periapical lesion. Oral Surg Oral Med Oral Pathol 1994;77:655–61.
26. Chen CP, Hertzberg M, Jiang Y, Graves DT. Interleukin-1 and tumor necrosis factor receptor signaling is not required for bacteria-induced osteoclastogenesis and bone loss but is essential for protecting the host from a mixed anaerobic infection. Am J Pathol 1999;155:2145–52.
27. Zhang X, Peng B. Immunolocalization of receptor activator of NF kappa B ligand in rat periapical lesions. J Endod 2005;31:574–7.
28. Kawashima N, Suzuki N, Yang G, et al. Kinetics of RANKL, RANK and OPG expressions in experimentally induced rat periapical lesions. Oral Surg Oral Med Oral Pathol Oral Radiol Endod 2007;103:707–11.